Dynamics of multiplayer games on complex networks using territorial interactions

Pedro H. T. Schimit[*]

Informatics and Knowledge Management Graduate Program, Universidade Nove de Julho, Rua Vergueiro, 235/249, CEP 01504-000, São Paulo, São Paulo, Brazil

Karan Pattni[†]

Department of Mathematical Sciences, University of Liverpool, Mathematical Sciences Building, Liverpool L69 7ZL, United Kingdom

Mark Broom[‡]

Department of Mathematics, City, University of London, Northampton Square, London EC1V 0HB, United Kingdom

The modeling of evolution in structured populations has been significantly advanced by evolutionary graph theory, which incorporates pairwise relationships between individuals on a network. More recently, a new framework has been developed to allow for multiplayer interactions of variable size in more flexible and potentially changing population structures. While the theory within this framework has been developed and simple structures considered, there has been no systematic consideration of a large range of different population structures, which is the subject of this paper. We consider a large range of underlying graphical structures for the territorial raider model, the most commonly used model in the new structure, and consider a variety of important properties of our structures with the aim of finding factors that determine the fixation probability of mutants. We find that the graphical temperature and the average group size, as previously defined, are strong predictors of fixation probability, while all other properties considered are poor predictors, although the clustering coefficient is a useful secondary predictor when combined with either temperature or group size. The relationship between temperature or average group size and fixation probability is sometimes, however, nonmonotonic, with a directional reverse occurring around the temperature associated with what we term "completely mixed" populations in the case of the hawk-dove game, but not the public goods game.

I. INTRODUCTION

Evolutionary graph theory is an important methodology for considering evolution in a population with structure, where certain groups of individuals are more likely to interact than others, for example due to geographical proximity or social status. It considers the evolution of a population of individuals in which each interacts with its neighbors through a graphical structure, and these interactions affect individual fitness and how the population updates, with replacements occurring between neighboring pairs. The population structure, i.e., its topology, can strongly affect its evolution [1–7]. Instead of considering homogeneously structured infinite populations, as is common in evolutionary game theory [8–10], inhomogeneous populations are considered. Interactions are generally pairwise, using standard games such as the prisoner's dilemma and the hawk-dove game [11–13]. We note that finite and/or spatial populations have previously been considered in different ways; for example [14,15] considered the spatial evolution of cooperative behavior, [16] considered a finite population whose members play a hawk-dove game, and [17] considered a hawk-dove game on a lattice.

Evolutionary graph theory generally considers pairwise interactions on a fixed graph structure between individuals along graph edges, although it is possible to consider multiplayer games through grouping all neighbors of an individual. This nevertheless generally involves certain groupings of fixed size [18]. For many species, animals live either alone or in distinct groups on a territory, which can vary considerably in size over time, and often overlaps with other territories. The same place can thus be used by one, two, or many individuals that will interact and sometimes compete, with the size and composition of the competing group varying significantly; examples include African wild dogs [19] or roadrunners [20]. Groups can be large cooperative units—for example, ant colonies. Primate groups can also be quite large, including conflicts over dominance and resource division. Such groupings can be even more complex and varied in human society.

To model such situations, evolutionary games with more than two individuals are needed. Such multiplayer games were introduced by [21] in biological problems and theoretically expanded by [22] and [23]; more recent modeling work has also been considered in [24], [25], and [10], chapter 9. A multiplayer hawk-dove game was introduced in [26], and public goods games have been considered in a number of papers [27–34].

Thus there is a need for models of evolution on structured populations that incorporate multiplayer games of varying

───────

[*]schimit@uni9.pro.br

[†]k.pattni@liverpool.ac.uk

[‡]mark.broom@city.ac.uk

032306-1

numbers of players. Broom and Rychtář developed a general framework for analyzing such multiplayer games in structured populations in [26], with further work on this in [35–38]. In particular, [36] considered evolution using three classical game scenarios (hawk-dove, prisoner's dilemma, and fixed fitness) in structured populations using the invasion process dynamics for some simple cases, using the "territorial raider" model, which used an underlying graphical structure as its basis [39].

In this paper we develop the above work to consider evolution on a large range of complex networks with a range of structural properties. Complex networks have previously been used in population evolution by using scale-free graphs and lattices [6,11,29,40], and random [11] and regular networks [29,41]. Although these models consider topological properties of the mentioned networks, they do not explore a wide range of topological parameters and structures, which is the focus in this paper. By considering complex network models [42], we attempt to use topological parameters and different structures to analyze how they are related to the fixation probability of mutants. Five types of complex network are considered in this paper: the Erdös-Renyi (random) network, small-world, scale-free, random regular, and Barábasi-Albert.

In general throughout the paper we shall use the alternative term "network" in place of "graph"; they are interchangeable, except that we wish to emphasize that the graphs or networks that we use represent the population in a way that is distinct to that of a graph in evolutionary graph theory (we shall only use "graph" for the evolutionary graph which describes how the population updates).

We will see throughout the paper that in order to simulate the model in a full range of different networks and population parameters, we had to run about ten billion different simulations. An analytical analysis in these circumstances is hard to describe, and a numerical process had to be formalized to get the results in an acceptable computational time, which is a critical point in the area [4,43] for either a large number of cases or big populations.

In Sec. II we outline the population model used in this paper, before describing the computational methodology in Sec. III and our results in Sec. IV. We conclude with a discussion of the paper and suggestions for future work in Sec. V.

II. THE MODELING FRAMEWORK

The modeling framework is given in full generality in [26]. It incorporates three key components: the population structure, the evolutionary dynamics, and the evolutionary game. In particular the general population structure is very flexible. Below we describe an important special case, which will be the basis of the work in this paper.

A. The fully independent model

A population contains N individuals $I_1, \ldots, I_N$ who are able to move around M places $P_1, \ldots, P_M$. The probability of individual I_n being at place P_m is denoted by p_{nm}; see Fig. 1 for a visual representation using a bipartite network. Based on discrete time, at each time step of the simulation, all individ-
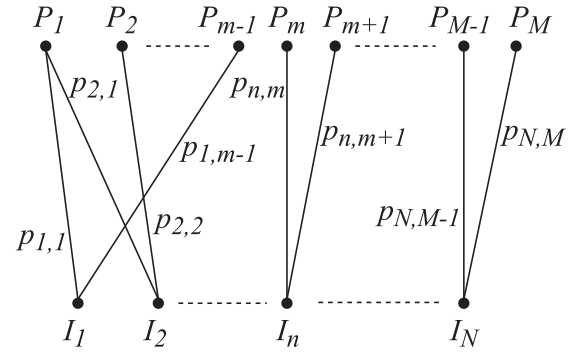

FIG. 1. The fully independent model from [26]. There are N individuals who are distributed over M places such that I_n visits place P_m with probability p_{nm}. Individuals interact with one another when they meet; for example, I_1 and I_2 can interact with one another when they meet in P_1.

uals move following their given distribution, resulting in the formation of groups at the different places (the group formed is simply the collection of all individuals at the given place). Letting $\mathcal{G}$ denote any group of individuals, the probability $\chi(m, \mathcal{G})$ that group $\mathcal{G}$ forms in place P_m is given by

$$\chi(m, \mathcal{G}) = \prod_{i \in \mathcal{G}} p_{im} \prod_{j \notin \mathcal{G}} (1 - p_{jm}). \tag{1}$$

When a group of individuals is formed they play a multiplayer game, and individual I_n will receive a payoff that depends on the group $\mathcal{G}$ it is present in and the place P_m occupied by this group, denoted by $R_{n,m,\mathcal{G}}$. Individual I_n's fitness is then calculated by averaging its payoffs over all possible groups and places, which is given by

$$F_n = \sum_m \sum_{\substack{\mathcal{G} \\ n \in \mathcal{G}}} \chi(m, \mathcal{G}) R_{n,m,\mathcal{G}}. \tag{2}$$

The fully independent model is still very general, and different examples were introduced in [26]. Perhaps the most important one of these was the territorial raider model, which was further developed in [36] and is the basis of the work in this paper.

B. The territorial raider model

In the territorial raider model of [26], a population of N individuals $I_1, \ldots, I_N$ can move to, and interact at, N different places $P_1, \ldots, P_N$; see Fig. 2(a). In particular it is assumed that individual I_n lives at place P_n and can also move to neighboring places; that is, individual I_n has place P_n as its original place, returning to it at the end of each iteration. The population is modeled using a network to represent this scenario, with nodes representing both individuals and places.

We assume that all individuals make moves which are independent of the moves of others, and also of the past movements of all individuals (including itself). The probability of an individual I_n being at place P_m at any time can thus be denoted by p_{nm}. The networks that we will study in later sections are thus representations of territorial raider models as described here, and not the standard graph as in evolutionary
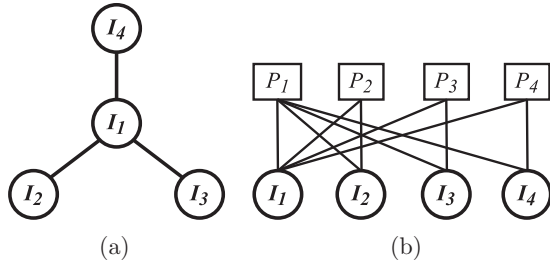
FIG. 2. (a) Population structure represented using a network where nodes represent individuals and places. Individual I_n lives in place P_n and can visit any neighboring places. For example, the home place of I_1 is place P_1 but it can visit places P_2, P_3, and P_4. (b) An alternative visualization on a bipartite network where individuals and places are clearly separated.

graph theory; i.e., they relate to the general representation as shown in Fig. 2(b).

We could allow each individual I_n to have a distinct movement distribution $(p_{nm})_{m=1,...,N}$, but this would generate (up to) $N - 1$ independent movement parameters for each individual, and make comparison between different networks difficult. We instead use a natural model in which a single parameter h governs every movement, so that an individual with d neighbors stays at its home node with probability $h/(h + d)$ and moves to the node of a given one of its neighbors with probability $1/(h + d)$; that is, the individual does not move with probability $h/(h + d)$ and moves with probability $d/(h + d)$. We term h the *home fidelity* parameter, as it is a measure of an individual's preference for its home node. For high home fidelity, individuals do not move much and will usually be alone; for low values they move a lot, and there is usually a lot more interaction within the population. Note that choosing $h = 1$ means that all allowable places, including the home node, are visited with equal probability.

C. Evolutionary dynamics

An evolutionary graph [1,44] is a graph with a weighted adjacency matrix $\mathbf{W} = (w_{ij})$, where $w_{ij} \geqslant 0$ is the replacement weight, strongly influencing which individuals are more likely to replace which others. Often weights are right-stochastic, i.e., $\sum_j w_{ij} = 1$, and this is the case for the current paper. Every node v_n of the evolutionary graph is occupied by precisely one individual, and if $w_{ij} > 0$ then the individual on v_i can place a copy of itself in v_j to replace the existing individual. Weights are selected so that the graph is strongly connected, so there is a route between any pair of nodes.

In this paper, the evolution of the population is described using the invasion process [1], a birth-death process in which the selection happens in the birth event. This process is very commonly used in evolutionary graph theory, originating in [1], and was adapted to the modeling framework used here in [36]. In particular, an individual is chosen to give birth to an offspring with probability

$$b_i = \frac{F_i}{\sum_{n=1}^N F_n} \tag{3}$$

who then replaces one of its neighbors with probability

$$d_{ij} = \frac{w_{ij}}{\sum_{k=1}^N w_{ik}}. \tag{4}$$

There are other replacement dynamics that can be considered; for example, see [37,44] for a list of different evolutionary dynamics that can be used.

We shall define a *well-mixed* population as one where all replacement weights (except perhaps the self-replacement weights) take equal value.

The replacement weights used in this paper are based on the assumption that an offspring of individual I_i is likely to replace another individual I_j proportional to the time I_i and I_j spend together (note that the offspring of I_i can also replace I_i itself, and the probability that this happens is proportional to the time I_i is alone). The probability that I_i and I_j meet is given by summing $\chi(m, \mathcal{G})$ over all m such that $i, j \in \mathcal{G}$. When they meet, it is assumed that I_i will spend an equal amount of time with each other individual in group $\mathcal{G}$ and, therefore, we weight $\chi(m, \mathcal{G})$ with $1/(|\mathcal{G}| - 1)$ since there are $|\mathcal{G}| - 1$ other individuals. Note that this is consistent with the payoffs from our public goods game, as we define in Sec. II D, where each pairwise payoff equally contributes to the total payoff an individual receives. When $i = j$, we can sum $\chi(m, \mathcal{G})$ over all m such that $\mathcal{G} = \{i\}$. Here there is no need to weight $\chi(m, \mathcal{G})$ because I_i is alone. The replacement weights are therefore calculated as follows:

$$w_{ij} = \begin{cases} \sum_m \sum_{\substack{\mathcal{G} \\ i, j \in \mathcal{G}}} \frac{\chi(m, \mathcal{G})}{|\mathcal{G}| - 1}, & i \neq j, \\ \sum_m \chi(m, \{i\}), & i = j \end{cases} \tag{5}$$

Let $\mathcal{S}$ be a state of the population such that $n \in \mathcal{S}$ implies that node n is occupied by an individual of type A. There are two absorbing states $\emptyset$ in which there are no type A individuals, and $\mathcal{N} = \{1, 2, \ldots, N\}$, where all individuals are of type A. The probability that a population with initial state $\mathcal{S}$ is absorbed in state $\mathcal{N}$ is denoted $\rho_{\mathcal{S}}^A$, and is referred to as the *fixation probability* for state $\mathcal{S}$, most commonly when there is only one type A individual in $\mathcal{S}$, i.e., $\mathcal{S} = \{i\}$ for $i \in \mathcal{N}$. The probability $\rho_{\mathcal{S}}^A$ is obtained by solving

$$\rho_{\mathcal{S}}^A = \sum_{S' \subset \{1,2,...,N\}} P_{\mathcal{S}\mathcal{S}'} \rho_{\mathcal{S}'}^A, \tag{6}$$

where $P_{\mathcal{S}\mathcal{S}'}$ is the probability of transitioning from state $\mathcal{S}$ to $\mathcal{S}'$. Since there are N states with one type A individual in them, the average fixation probability ρ^A is taken, which is calculated as follows:

$$\rho^A = \frac{1}{N} \sum_{i=1}^N \rho_{\{i\}}^A. \tag{7}$$

We can similarly define the fixation probability for a type B individual.

The *temperature* of an individual was defined in [1] to measure how likely an individual will be replaced in the case of a neutral population in which all individuals have constant

fitness. The temperature is defined as follows:

$$T_j = \sum_{i=1, i \neq j}^{N} w_{ij}. \tag{8}$$

Note that the higher the temperature of an individual, the more likely that that individual will be replaced. In a homogeneous population structure, such as a complete network, each individual will have the same temperature.

D. Multiplayer games in structured populations

In this section we shall describe three multiplayer games, the public goods game, the hawk-dove game, and the "game" with fixed fitnesses. In each game we will consider a contests between two different types of individual, A and B, and we will later consider the fixation probability of a single A in a population of Bs as well as the fixation probability of a single B in a population of As.

1. The multiplayer hawk-dove game

A population consists of hawks, which we label A, and doves, which we label B. All individuals that meet on a place play a multiplayer hawk-dove game, competing for a single reward V. If all of these individuals are doves, they divide the reward equally among themselves. If there are one or more hawks, the doves concede and then all of the hawks fight, with the winner getting the reward, while the others receive a cost C. In addition, all individuals receive R as a background reward, representing the reward gained from other activities. Therefore, for a single game involving a group of a hawks and b doves, the average payoffs for the hawks and the doves, respectively, are

$$R_{a,b}^A = R + \frac{V - (a-1)C}{a}, \tag{9}$$

$$R_{a,b}^B = \begin{cases} R, & \text{if } a > 0, \\ R + \frac{V}{b}, & \text{if } a = 0. \end{cases} \tag{10}$$

We note that the classical two-player hawk-dove game is just a special case of our game as defined. For the two-player game for the infinite well-mixed population there is a unique mixed evolutionarily stable strategy (ESS) if $V < C$, and otherwise pure hawk is the unique ESS. For a fixed group size n this condition becomes $V < (n-1)C$, and depends on the distribution of the group size when this is variable, as in our case. The parameter values we have used in this paper ($V = 2$, $C = 1$) would thus favor hawks for the 2-player game, but not necessarily for larger groups.

2. The public goods game

Here a population consists of cooperators, A, and defectors, B. They again start with a background payoff R, and then play a public goods game among all of the individuals on a given place. Following [33], a cooperator pays a cost C so that other individuals in the group share the benefit V. We note that we assume that this cost is always paid even if the cooperator is alone. Whether this is in fact the case would depend on the precise nature of the biological scenario, and it would have been equally plausible to assume that for lone

individuals the cost is not paid. An interesting alternative way of considering lone individuals was also modeled in [45]. The method that we use is consistent with that used in [36] and makes the evolution of cooperation harder to achieve than if this was not the case, and this game is thus a tougher test of when cooperation can evolve than alternatives. We also note that no similar ambiguity about lone individuals exists for the hawk-dove game above, where the payoff to lone individuals is a natural extension of the contested game.

A single game involving a group of a cooperators and b defectors, yields, respectively, average payoffs for cooperators and defectors of

$$R_{a,b}^A = \begin{cases} R - C, & a = 1, b = 0, \\ R - C + \frac{a-1}{a+b-1}V, & \text{otherwise,} \end{cases} \tag{11}$$

$$R_{a,b}^B = R + \frac{a}{a+b-1}V. \tag{12}$$

3. Fixed fitness case

For the fixed fitness game, fitness is frequency-independent and individuals do not really interact with each other but simply receive a constant payoff depending only on their type, independently of the composition of the group. For a group of a individuals of type A and b individuals of type B, we define

$$R_{a,b}^A = R + V, \tag{13}$$

$$R_{a,b}^B = R. \tag{14}$$

E. Evolutionary graph theory and complex networks

As discussed in Sec. II B, the territorial raider model that we use is based on an underlying network structure, and different network structures can yield very different results, for example in terms of fixation probability. We shall consider a range of such networks in this paper, and here we discuss these, together with a few important network properties.

Erdös and Rényi [46] formulated a random network model, where n nodes are connected by e edges randomly chosen among the $n(n-1)/2$ possible edges, so that the network contains a fraction $q = e/[n(n-1)/2]$ of possible edges (this fraction of existing edges is also called the *density*). Watts and Strogatz [47] proposed a model with similar average shortest path length to the Erdös-Rényi network (usually small), which can also aggregate nodes in clusters. Consider a regular network with each node connected to m close individuals; then rewire a fraction p of the connections. It creates a *small-world* network, mainly locally connected with long-distance random connections. When $p = 1$, the network is totally random, as for the Erdös-Rényi model.

Such an aggregation of nodes is measured by the *clustering coefficient*. Consider a node i of the network; then the clustering coefficient c_i for the node i is the fraction of existing connections among these neighbors and the total possible, and the average clustering coefficient is given by $\bar{c} = (1/n) \sum_{i=1}^{n} c_i$ [47].

Some real networks have the property of *the rich get richer*; that is, nodes that are introduced into the network are more likely to connect with nodes that have a high number of connections (the *degree* of a node). The *degree distribution*
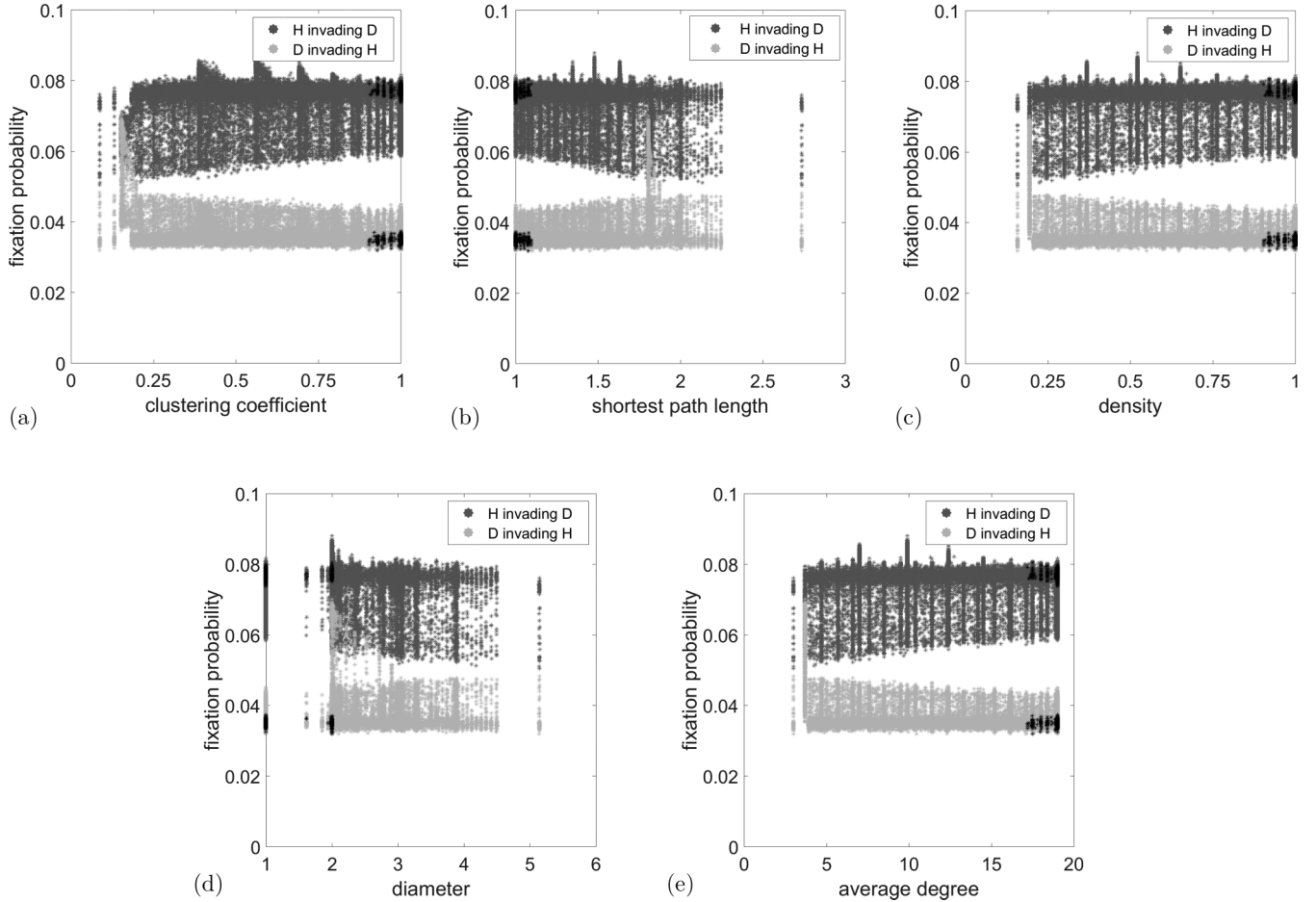
FIG. 3. Fixation probability as a function of (a) clustering coefficient, (b) shortest path length, (c) density, (d) diameter, and (e) average degree for all network simulations for the hawk-dove game. The dark gray dots represent the case of H invading D, the light gray dots represent the case of D invading H, and for both cases, black dots represent simulations with well-mixed networks. The parameter values are $R = 10$, $C = 1$, $V = 2$.

of these networks follows the expression $\pi(k) \sim k^{-\gamma}$, with $\gamma \simeq 2.2$ [48,49]. A distribution of nodes $\pi(k) = Ak^{-\gamma}$, with A and k constants, is termed *scale-free* [50]. Deriving from the scale-free model, Barabási and Albert [51] proposed a different rule: *preferential attachment*, where the probability π_{ba} that a new node will connect to a node i is a proportional to k_i, the degree of i, that is, $\pi_{ba}(k_i) = k_i / \sum_{j=1}^{n} k_j$.

III. METHODOLOGY

The networks are representations of territorial raider models. We will consider five models of undirected networks: Erdös-Rényi, small-world, Barabási-Albert, scale-free, and regular, with fixed size of $N = 20$ nodes. The parameters forming the networks will be varied accordingly in order to provide the widest topological range within a model. The library iGraph [52] generates the networks and returns the topological properties.

For the Erdös-Rényi network, the only parameter used as an input is the fraction of connections. Therefore, m_{er} is varied for the values $m_{er} = 0.2, 0.205, 0.21, 0.215, \ldots, 1$, generating 161 types of random network. For small-world, the

number of close neighbors connected to each node m_{sw} and the fraction of rewired connections p_{sw} are the input parameters, and the ranges of each parameter are $m_{sw} = 2, 4, \ldots, 18$ and $p_{sw} = 0.05, 0.01, \ldots, 1$ generating 180 different types of network.

The Barabási-Albert networks also have two input parameters: m_{ba} is the number of connections generated per node, and γ_{ba} the exponent of the probability of a node i with degree k_i being chosen to get an edge $\pi_{ba}(k_i) = (k_i / \sum_{j=1}^{n} k_j)^{\gamma_{ba}}$ according to the nonlinear preferential attachment. When $\gamma_{ba} = 1$ we have the linear and traditional form of the Barabási-Albert model [51]. Therefore, these parameters are varied according to $m_{ba} = 2, 4, \ldots, 18$ and $\gamma_{ba} = 1, 1.2, 1.4, \ldots, 5$, generating 189 different types of networks.

The scale-free networks also have the exponent γ_{sf} as an input, as well as q_{sf}. The first is the exponent of the power law distribution $\pi(k_i) \sim k_i^{-\gamma}$ of the network, and the second is the percentage of total edges to be added to the network. Therefore, we used the values $q_{sf} = 0.25, 0.25, 0.3, \ldots, 1$ and $\gamma_{sf} = 2, 2.25, 2.5, \ldots, 5$, generating 208 types of networks. In this case, the configuration model used by iGraph is described in [53].
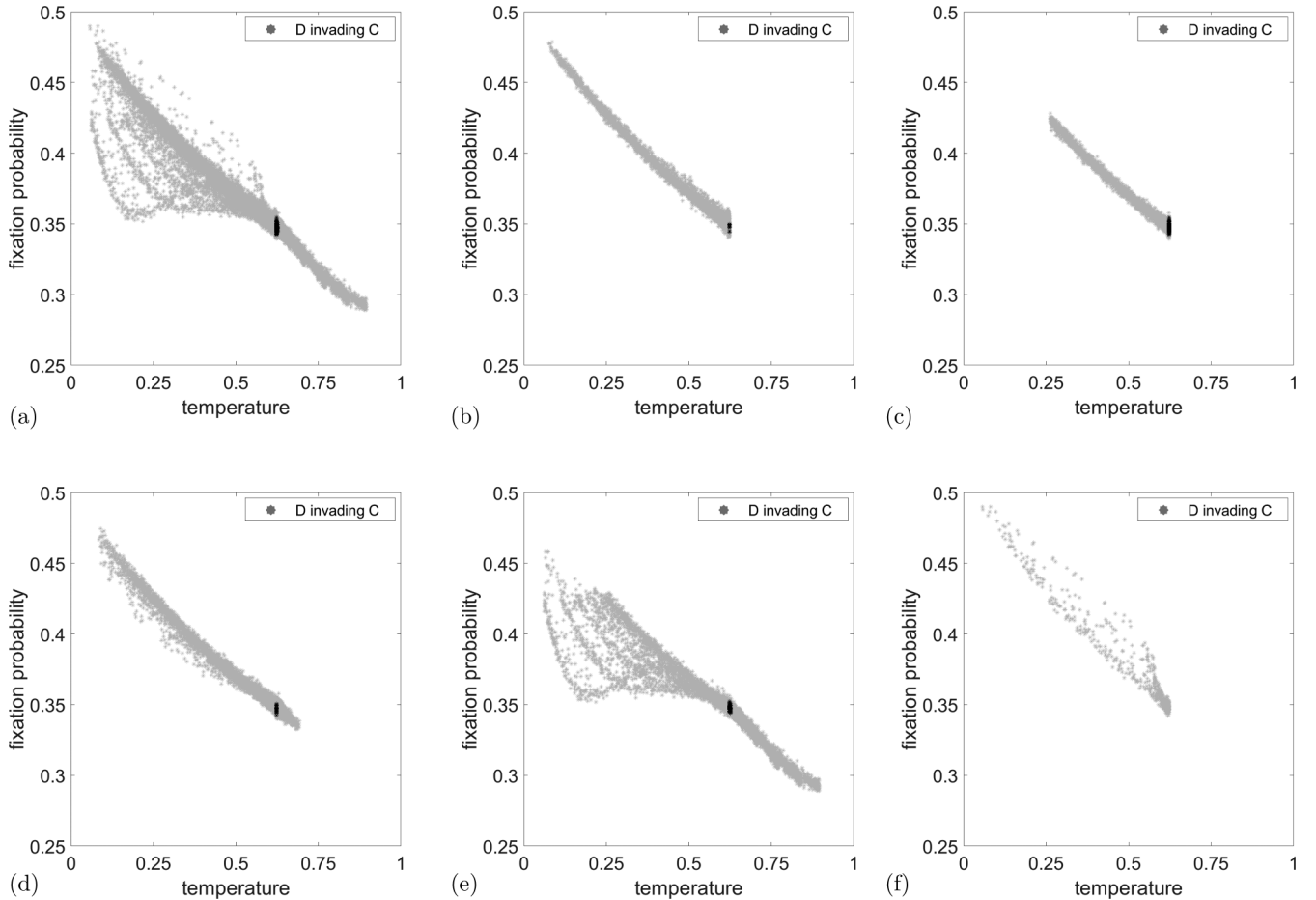
FIG. 4. Fixation probability as a function of temperature considering the public goods game for (a) all networks, (b) Erdös-Rényi, (c) small-world, (d) scale-free, (e) Barabási-Albert, and (f) random regular networks. For the selected parameters, the fixation probability for C invading D is effectively zero in all cases, so we have omitted these results. The light gray dots represent the case of D invading C and the black dots represent simulations with well-mixed networks. The parameter values are $R = 2$, $C = 1$, $V = 2$.

For regular networks, the only input parameter for generating the network is the degree of each node, which varies in the interval $k = 3, 4, \dots, 19$, and we have 17 types of networks.

Each combination of the three games described in Sec. II D with two situations per game (the invasion of a randomly placed individual of each type placed into a population of the other type) as simulated for each type of network listed previously. Moreover, in order to have enough variation for h, 50 simulations with random h were run for each combination of games and situations and each type of network, giving 226 500 cases. The value of h is randomly chosen in the interval $0.01 \leqslant h \leqslant 100$ uniformly distributed on the logarithmic scale.

One simulation is delineated as follows:

(1) Given the parameters, a network is formed using iGraph.

(2) The mutant is randomly put on one of the nodes.

(3) Each individual moves (or not) from its home place according to the model. Every group with one or more individuals plays the multiplayer game.

(4) Each individual moves (or not) from its home place according to the model. Run the birth-death process: Randomly pick an individual proportional to its fitness, and it replaces a

random individual from the group it is in; if it is alone, there is no replacement.

(5) The simulation ends when either individuals A or B dominate the population.

(6) This process is run 50 000 times to minimize the statistical variability of the results [95% confidence intervals of estimates always have width (sometimes much) less than 0.01].

Note that we use the typical initial condition called uniform initialization [54]; that is, all nodes have the same probability to have the initial mutant, in order to maintain consistency with the previous work [36]. There is also an alternative method called temperature initialization; see for example [55].

IV. RESULTS

The aim of our analysis is to find good predictors of the key properties of our evolutionary process, concentrating on the most important, the fixation probability. When dealing with complex networks, the first objective is often to analyze the dynamical properties of the system with topological parameters. However, in the model presented, the standard parameters, including the clustering coefficient, shortest path length,
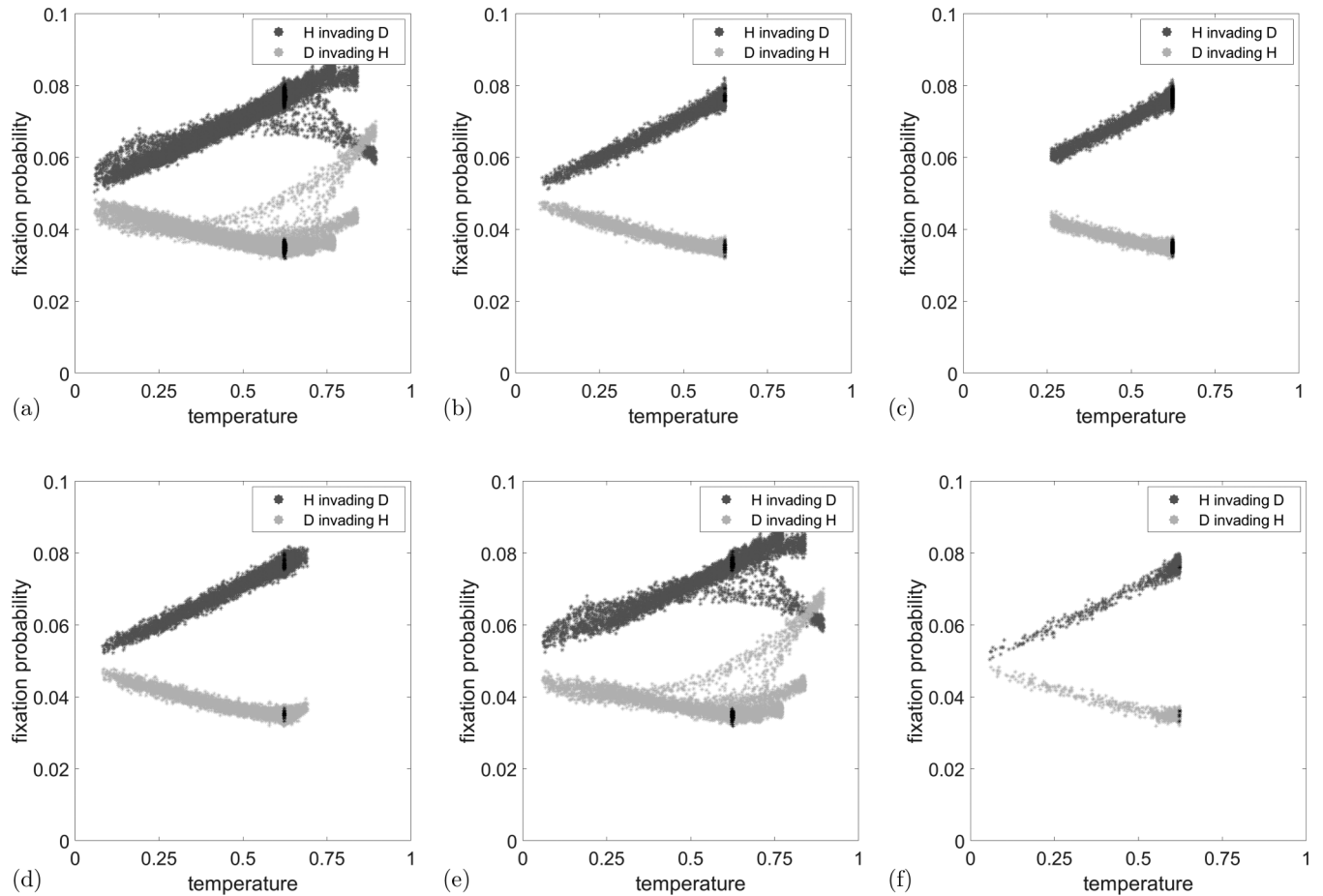
FIG. 5. Fixation probability as a function of temperature considering the hawk-dove game for (a) all networks, (b) Erdös-Rényi, (c) small-world, (d) scale-free, (e) Barabási-Albert, and (f) random regular networks. The dark gray dots represent the case of H invading D, the light gray dots represent the case of D invading H, and for both cases, black dots represent simulations with well-mixed networks. The parameter values are $R = 10$, $C = 1$, $V = 2$.

density, and diameter, seem to give very little information about the fixation probability. We can see this in the case of (a) clustering coefficient, (b) shortest path length, (c) density, and (d) diameter for all network simulations for the hawk-dove game in Fig. 3. The cases for all networks separately, and also for the other two games in combination with each of the networks, are similar. However, as we shall see, the clustering coefficient does have an important secondary role to play.

Note that from here, we will use the original letters of the game's strategies: for the public goods game, C for cooperators and D for defectors, and for the hawk-dove game, H for hawks and D for doves.

For small networks [36], we have already seen that the temperature is a good predictor of the fixation probability. Thus we considered it for this far wider range of (and, with 20 nodes, larger) networks. The temperature is similarly a good predictor over the range of possibilities that we have considered. Figures 4, 5, and 6 show the fixation probability as a function of temperature for (a) all networks, (b) Erdös-Rényi, (c) small-world, (d) scale-free, (e) Barabási-Albert, and (f) random regular networks, for our three games, the public goods game, hawk-dove game, and the fixed fitness

case, respectively. Moreover, Figs. 7, 8, and 9 show the fixation probability as a function of average group size for the same cases.

In this paper we consider the group size from the individual's perspective, as opposed to from the observer's perspective; see [36] (in [56] these were referred to as the "experienced group size" and simply the group size, respectively). For example, if half of all groups are of size 2 and half are of size 6, then 3/4 of individuals are in groups of size 6, so the mean from the individual's perspective is 5, but from the observer's perspective is 4.

In our figures we have tried to pick out sets of parameters that yield interesting results. There are many combinations of games and parameters in which one of the strategies is completely dominant for all networks, or in which there is no appreciable difference across the networks, so that the effects are drowned out by the statistical variability due to our simulations. This is in fact a useful observation; for networks generated in the different random ways that we do, there is often no appreciable difference between fixation probabilities over the full range of networks, and interesting differences that can be found may be due to quite exceptional constructed networks, which while of interest lack general applicability.
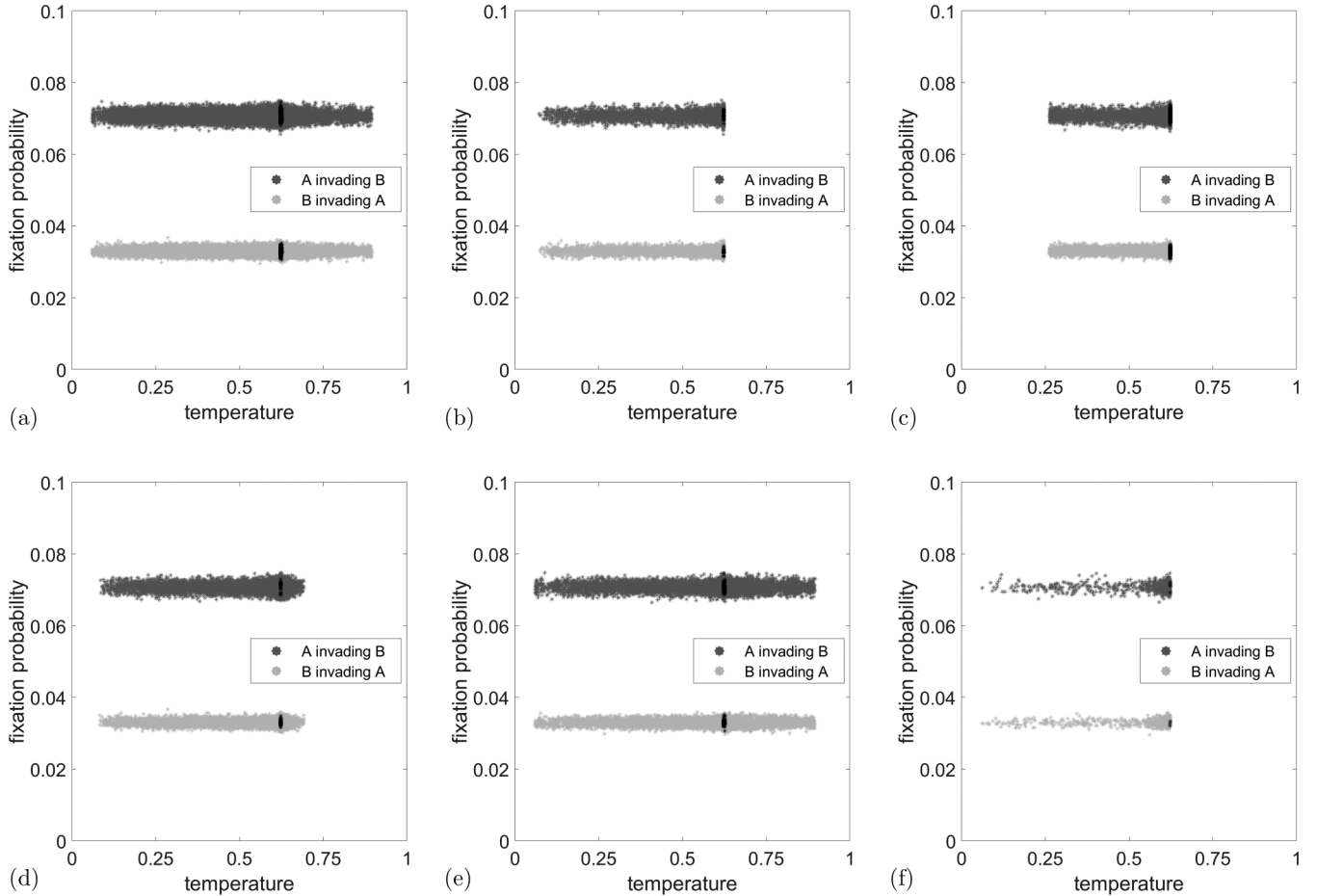
FIG. 6. Fixation probability as a function of temperature considering the fixed fitness game for (a) all networks, (b) Erdös-Rényi, (c) small-world, (d) scale-free, (e) Barabási-Albert, and (f) random regular networks. The dark gray dots represent the case of A invading B, the light gray dots represent the case of B invading A, and for both cases, black dots represent simulations with well-mixed networks. The parameter values are $R = 50$, $C = 1$, $V = 2$.

For the public goods game we could not find a marked network effect in cases in which each strategy could reasonably invade the other, so a nonflat line could only be found for one strategy to invade at the expense of the other. Thus in Figs. 4 and 7, the probability of C invading D is small for all networks leading to a flat line close to zero, so we have omitted this and plotted a range of values on the *y* axis to better illustrate the more interesting case of D invading C. For hawk-dove games there was interesting behavior for many parameters, so we have simply chosen parameters as in [36] in Figs. 5 and 8. Finally for the fixed fitness case there was no interesting behavior, and we have simply selected parameters that feature both fixation probabilities clearly on the graph in Figs. 6 and 9, but these flat lines happened in all cases.

It is worth noting that in panel (e) of Figs. 4–9, Barabási-Albert networks have the wider range of fixation probability and temperature values and their curves are thus almost the same as for the all-network data [panel (a) of Figs. 4–9].

In Fig. 4 we see that for the public goods game there is a strong linear trend for the fixation probability in terms of the temperature for all networks, and a straight-line fit would be accurate over the full range for the majority of the networks. However there are some outlying networks, and the Barabási-Albert networks in particular yield some very

unusual behavior for the lower temperatures. We shall revisit this interesting feature in Sec. IV B below.

The hawk-dove game in Fig. 5 similarly yields nice straight-line fits for the fixation probability in terms of the temperature for all network types except again for Barabási-Albert networks, and to some extent scale-free networks. For hawks invading a dove population this is an increasing trend, but for a dove invading a hawk population a decreasing one. For Barabási-Albert and scale-free networks the trend is reversed at around the completely mixed temperature, marked by the black dots (see Sec. IV A) for invading doves, and a value somewhat higher than that for the invading hawks. This is complicated by the split in the trend in the case of Barabási-Albert networks, where a branch breaks off the main trend in at least two places for both types of individual; we shall investigate this phenomenon in more detail in Sec. IV B.

The fixed fitness game simply yields flat lines in Fig. 6. There is some between-network variation, not simply due to simulation statistical errors, but the temperature is not useful in predicting these at all.

Figure 7 shows a clear relationship between fixation probability and average group size for the public goods game. Figure 8 shows a similar relationship between fixation probability and average group size for the hawk-dove game. We discuss
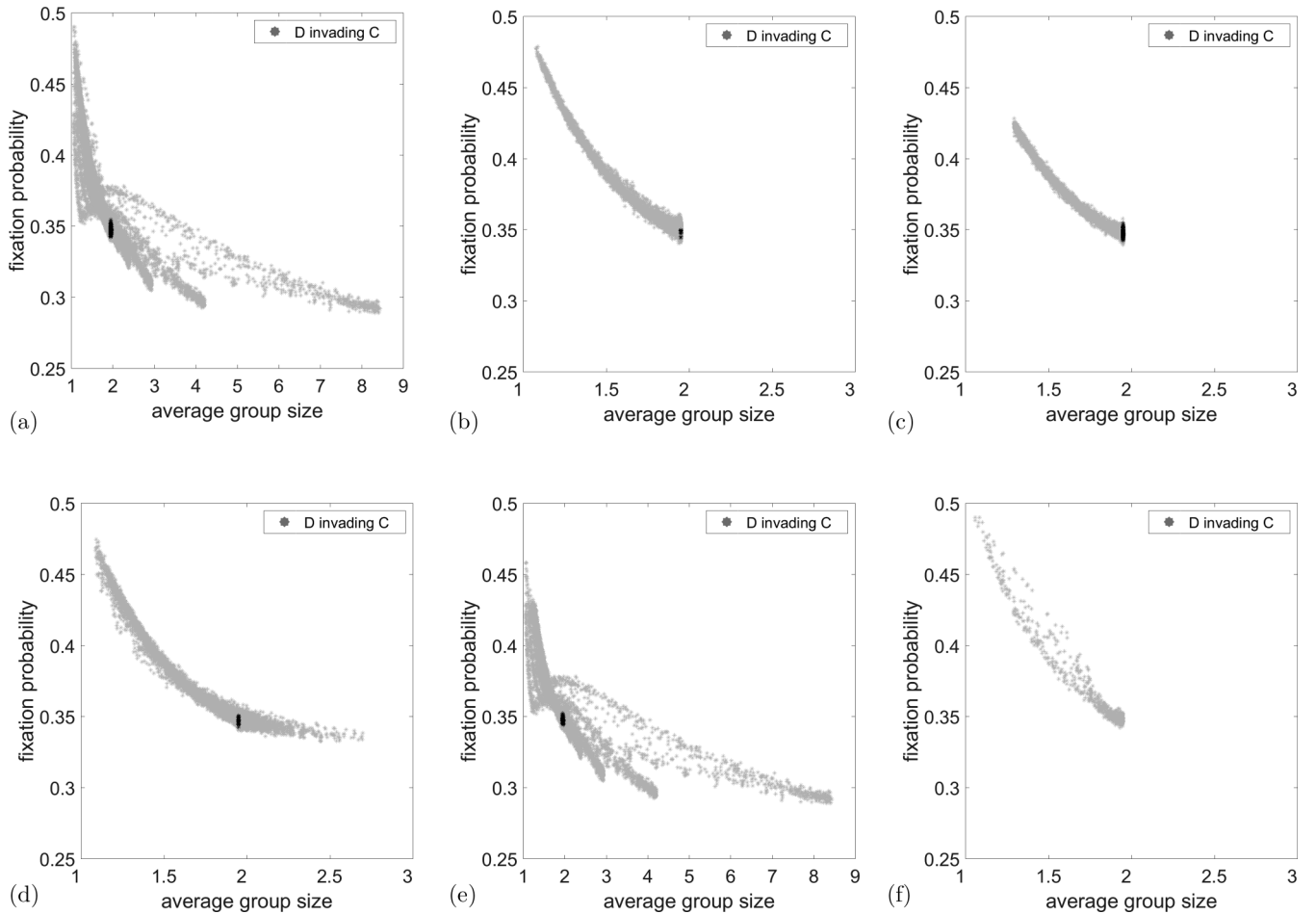
FIG. 7. Fixation probability as a function of average group size considering the public goods game for (a) all networks, (b) Erdös-Rényi, (c) small-world, (d) scale-free, (e) Barabási-Albert, and (f) random regular networks. The light gray dots represent the case of D invading C and black dots represent simulations with well-mixed networks. The parameter values are $R = 2$, $C = 1$, $V = 2$. The C invading D situation is a flat line close to 0.

the interesting issues above in Sec. IV B. We see similar flat lines to before for the fixed fitness case in Fig. 9. In general average group size and temperature are strongly correlated, so it is not a surprise to see a similar relationship here.

Linearity with the temperature can partly be explained by the fact that for the models in this paper an individual's temperature effectively reduces to the probability of it not being alone at the replacement event and in the contests that lead to payoffs (note that these two need not be the same [38] and that a more complex temperature concept was needed when subpopulations formed on nodes [37]). Thus for small temperatures, mean temperature is strongly correlated with the intensity of selection, and the fixation probabilities are close to straight lines at a temperature of 0. This can be most clearly seen for the hawk-dove game, where lone individuals of both types gain reward V and the intercept with the y axis is simply $1/N = 1/20$. This is also true for the public goods game, though here the y axis intercept is around $1/2$, which occurs since lone cooperators and defectors have different rewards. For our chosen parameter values the defectors have twice the fitness of the cooperators, and the value of (actually marginally above) $1/2$ is that obtained from the classical Moran process. It is remarkable here, however, that even for

quite low temperatures there is quite a variety in fixation probabilities; i.e., this linear relationship breaks down quite quickly.

A. Well-mixed and completely mixed populations

A *well-mixed* population was previously defined in Sec. II C as one where all replacement weights (except perhaps the self-replacement weights) take equal value. For the territorial raider model with movement controlled by the single home fidelity parameter h this happens whenever the network is complete. There is a stronger criterion, namely a *completely mixed population* that occurs when $h = 1$.

The temperature at a given node, as stated in Sec. II C, in the territorial raider model is the probability that that individual is not alone. For a complete network with $h = 1$, all individuals will have the same probability of being alone, and consequently the network temperature is simply given by

$$T_w = 1 - \left(1 - \frac{1}{n}\right)^{n-1} \approx 1 - e^{-1} = 0.632 \qquad (15)$$

(note that the value of the above formula for the case $n = 20$ used in this paper is $T_w = 0.623$). Networks with many
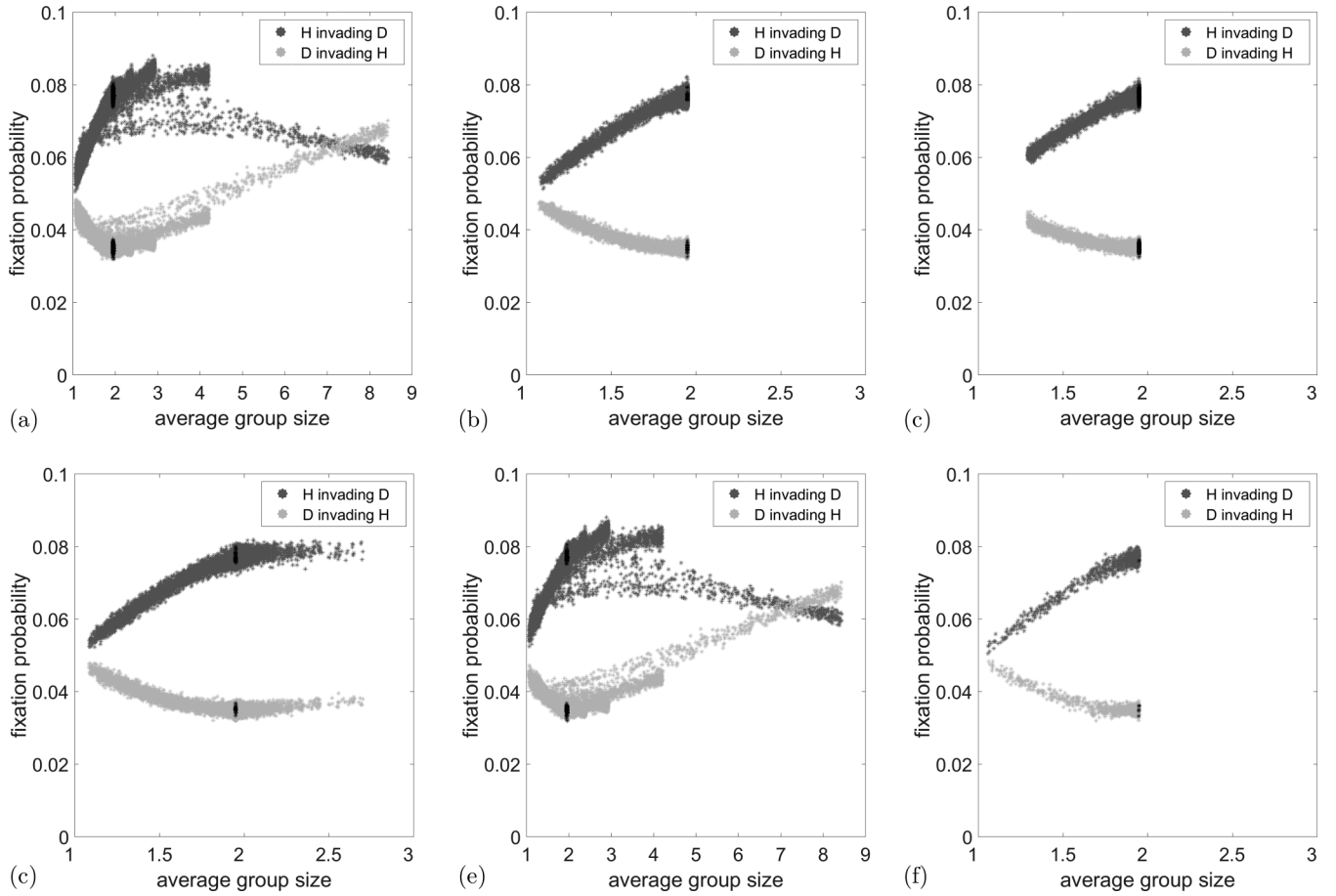
FIG. 8. Fixation probability as a function of average group size considering the hawk-dove game for (a) all networks, (b) Erdös-Rényi, (c) small-world, (d) scale-free, (e) Barabási-Albert, and (f) random regular networks. The dark gray dots represent the case of H invading D, the light gray dots represent the case of D invading H, and for both cases, black dots represent simulations with well-mixed networks. The parameter values are $R = 10$, $C = 1$, $V = 2$.

connections and h not too far from 1 will have temperatures close to this. We note that here the distribution of the number of an individual's group mates is approximately Poisson (1) and so for example the probability of groups of size 1, 2, 3, and 4 or more are 0.368, 0.368, 0.184, and 0.080, respectively. Here the mean group size is just 2, and so larger mean groups will present larger actual group sizes with higher probability.

Erdös-Rényi, small-world, and random regular networks have a maximum temperature of around 0.63, so that the temperatures of completely mixed populations are the maximum value found. The small average group size is due to the random (and uniform) distribution of connections that does not concentrate individuals in larger groups. Barabási-Albert networks and scale-free networks can reach higher temperatures and higher group sizes than the other types of networks, however. In general more irregular networks combined with low h can give higher temperatures; for example a star with $h = 0$ would yield a temperature of $1 - 1/n$, as the central individual would always be alone at another node, while all others would be together in the center. The black dots in Figs. 4 to 9 indicate cases where the population is close to being completely mixed. We have used randomly generated h values (and only a few of our networks were complete), so none of the selected networks are exactly completely mixed.

Thus we have marked networks in which $0.9 \leqslant h \leqslant 1.1$ and the density is higher than 0.9, since these are approximately completely mixed (and as we see, give close to the above completely mixed fixation probability).

Moreover, Barabási-Albert networks and to a small extent scale-free networks have a change in the temperature trend when the temperature is around 0.63 and average group size is around 2 in the case of the hawk-dove game. These values are related to well-mixed populations and are a threshold between networks of different character, where the higher temperature networks have connections concentrated on a few nodes and low clustering coefficients, as we discuss below.

B. Unusual network features

In this section we investigate some unusual features of our plots. In particular we consider two aspects. First, we ask why there is a turning point in the main trend for the hawk-dove game in Figs. 5(e) and 8(e). Second, we ask why on some plots there is a subset of networks that display completely different trends from the rest, in particular the two breakaway lines in Fig. 5(e) and the set of diverse trends for the low-temperature values in Fig. 4(e).
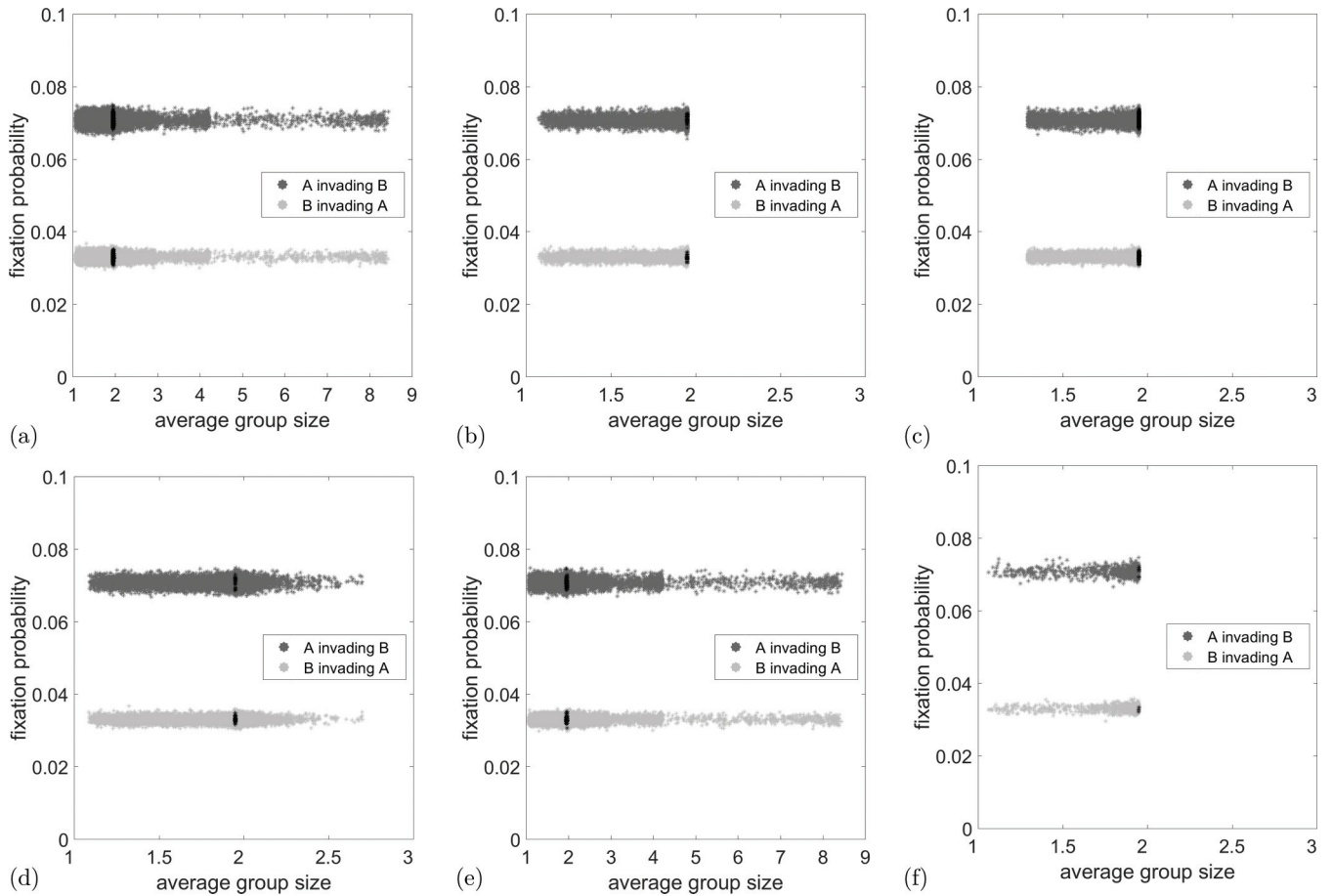
FIG. 9. Fixation probability as a function of average group size considering the fixed fitness game for (a) all networks, (b) Erdös-Rényi, (c) small-world, (d) scale-free, (e) Barabási-Albert, and (f) random regular networks. The dark gray dots represent the case of A invading B, the light gray dots represent the case of B invading A, and for both cases, black dots represent simulations with well-mixed networks. The parameter values are $R = 50$, $C = 1$, $V = 2$.

Tables I and II show the average standard deviation of the node temperature, average clustering coefficient, average iterations (number of iterations for either type of individual to dominate the population), average h, the average group size, and the average degree for different intervals of temperature for Barabási-Albert and scale-free networks, respectively. The interval $0.58 < t < 0.68$ is centered around where the turning point occurs for the hawk-dove game, and the intervals $t \leqslant 0.58$ and $t \geqslant 0.68$ display two distinct linear trends, separated by this turning point.

We can see from the tables that the midtemperature networks have both a higher clustering coefficient and lower standard deviation of the node temperature than for the lower and higher temperature networks. These midtemperature networks

are generally the best connected, which naturally leads to a higher clustering coefficient, at least in the types of networks that we have considered. These are also the networks closest to the completely mixed populations, where identical nodes lead to zero standard deviation in the node temperature. Thus in this range, this standard deviation is low.

We also see that higher temperature is correlated with larger group size. This can help explain the turning point for the hawk-dove game, where hawks do best (as invader or invaded population) compared to the other cases. In the cases that we consider hawks generally outperform doves, but for lone individuals the payoffs are the same. Thus for low temperature and so group size, hawk and dove fixation probabilities are not much different (each converging to 1/20,

TABLE I. Data for different temperature intervals for Barabási-Albert networks.

Temperature (t)	Average standard deviation of node temperature	Average clustering coefficient	Average iterations	Average h	Average group size	Average degree
$t \leqslant 0.58$	0.1009	0.65	227.1	34.08	1.53	11.91
$0.58 < t < 0.68$	0.0380	0.86	101.7	1.66	2.03	16.04
$t \geqslant 0.68$	0.1954	0.45	93.9	0.25	3.77	8.11

TABLE II. Data for different temperature intervals for scale-free networks.

Temperature (t)	Average standard deviation of node temperature	Average clustering coefficient	Average iterations	Average h	Average group size	Average degree
$t \leqslant 0.58$	0.0690	0.61	211.8	33.63	1.49	10.97
$0.58 < t < 0.68$	0.0373	0.67	102.8	1.11	1.98	12.26
$t \geqslant 0.68$	0.1263	0.41	99.2	0.04	2.56	5.58

since the population size is 20 as temperature converges to 0 and group size converges to 1). Similarly large groups can involve multiple hawk-hawk fights and so are also bad for hawks. There is thus an intermediate region where hawk performance is relatively at its highest.

Now consider the unusual patterns that depart from a linear trend in the earlier figures, in particular for the low temperatures for the public goods game from Fig. 4. In Fig. 10 we see a color-coded plot, where four of the key figures from before are repeated, but this time lighter dots represent higher clustering coefficients. Considering Fig. 10(a) we can clearly see the different lines for low temperature correspond to

different values of clustering coefficients in a very clear way. Higher clustering coefficients give the linear trend of fixation probability, while low values give the different patterns of low temperatures. The split into distinct lines here comes about from the way we chose our parameters for the Barabási-Albert model. For instance, the darkest line near low temperatures on Fig. 10(a) is related to the number of connections generated per node $m_{ba} = 2$, and the space between this trend and the next would be filled if we used $m_{ba} = 3$, since the next trend is related to $m_{ba} = 4$. We note that for higher temperatures there is less variability in the clustering coefficients, with all m_{ba} cases tending to the same a single trend line here.
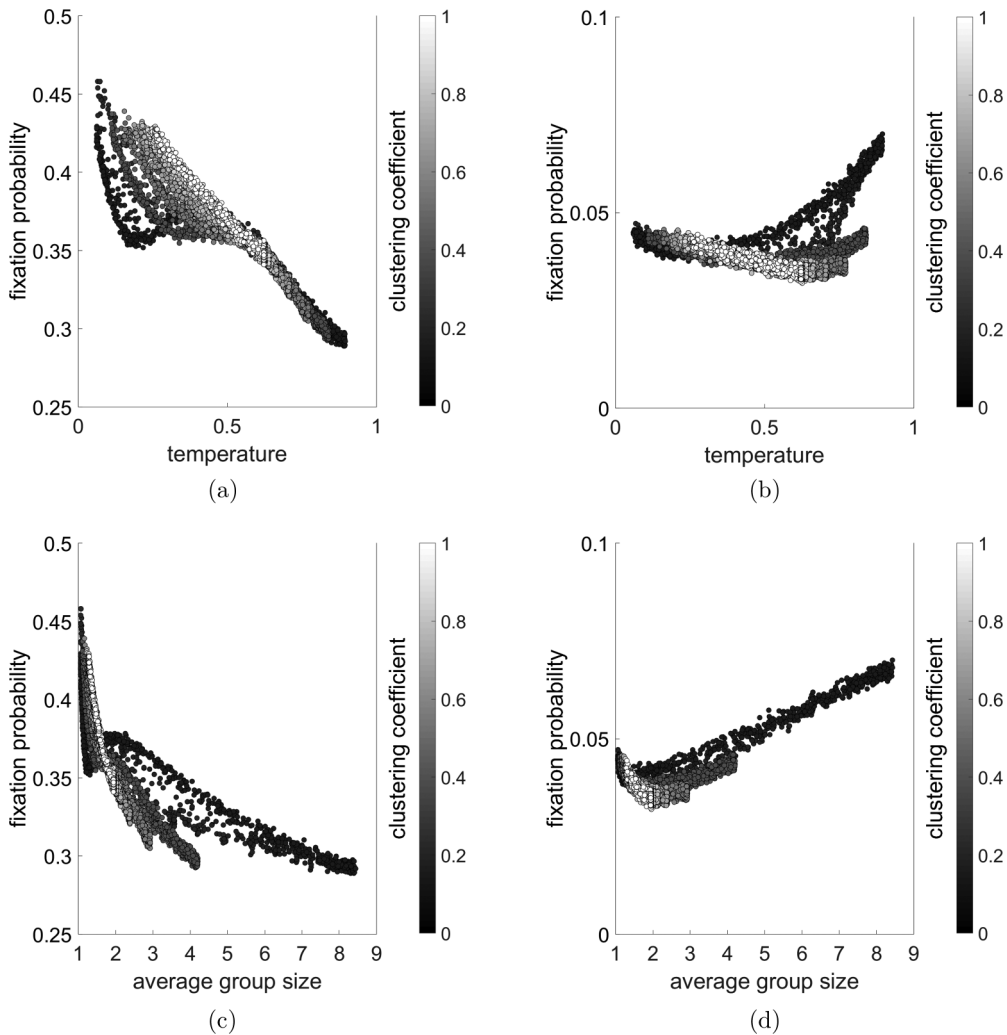

FIG. 10. Fixation probability as a function of temperature [(a) public goods game, (b) hawk-dove game] and average group size [(c) public goods game, (d) hawk-dove game] with a closer look at the clustering coefficient (see the vertical bar accompanying each figure), with D invading C and D invading H.
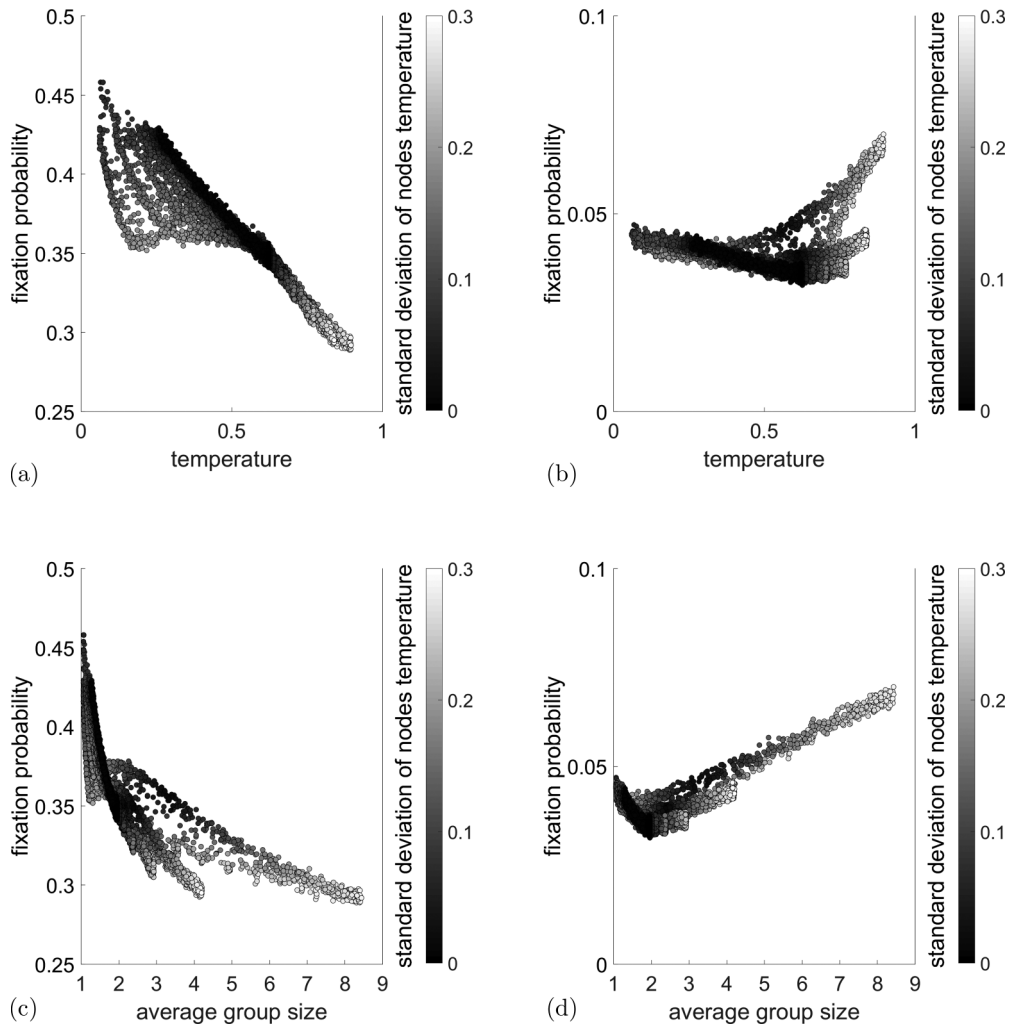
FIG. 11. Fixation probability as a function of temperature [(a) public goods game, (b) hawk-dove game] and average group size [(c) public goods game, (d) hawk-dove game] with a closer look at the standard deviation of node temperature (see the vertical bar accompanying each figure), with D invading C and D invading H.

Regarding Figs. 10(b)–10(d), the unusual patterns are always related to low clustering coefficient values. Comparing these results with Fig. 11, we can see that these points are also related to high values of the standard deviation of the node temperature. Note that for the hawk-dove game, the temperature trend starts to change where the standard deviation of the node temperature is high. For Figs. 10(c), 10(d), 11(c), and 11(d), for large average group size there are a few large groups, which decreases the clustering coefficient and increases the standard deviation of the node temperature.

Figures 10 and 11 are plotted by overlapping the dots. In this case, the data regarding low clustering coefficient are the first to be plotted, and high clustering coefficient data are in the front of the figure. Figure 12 shows a three-dimensional perspective of the same networks, adding the clustering coefficient in the new axis. Note that the low clustering coefficient trend (which would be all the very dark dots in Fig. 10) was hidden. The gaps between the curves are related to the parameters chosen to form the network. For instance, the curve with the lowest clustering coefficient is associated with $m_{ba} = 2$, followed by the curve with $m_{ba} = 4$, and so on.

We can see from Fig. 10 [and also from Figs. 12(a) and 12(c)] that for fixed group size, defectors perform better for the cases with a lower clustering coefficient, and so should allow for better mixing within the population, which is known to favor defectors. In addition, as we saw in Tables I and II, a lower clustering coefficient is associated with a higher standard deviation of node temperature and thus also with a more variable group size, and we see a consistent effect in Fig. 11. The advantage of defectors over cooperators in any given group is the size of the cost C (the only chance for cooperators to outperform defectors being in clustering preferentially with other cooperators), but the total payoff is smaller, and so the relative advantage larger, for lone individuals, with any group size above 1 that involves a cooperator being approximately equivalent. Thus defectors have the largest fixation probability when the probability of individuals being alone is largest, which occurs when the group size is most variable. More variable group sizes are similarly bad for hawks as we have discussed above, so there is a similar effect here with lower clustering coefficients favoring doves.

For a fixed temperature, group size increases with a decreasing clustering coefficient. Thus for a fixed temperature,
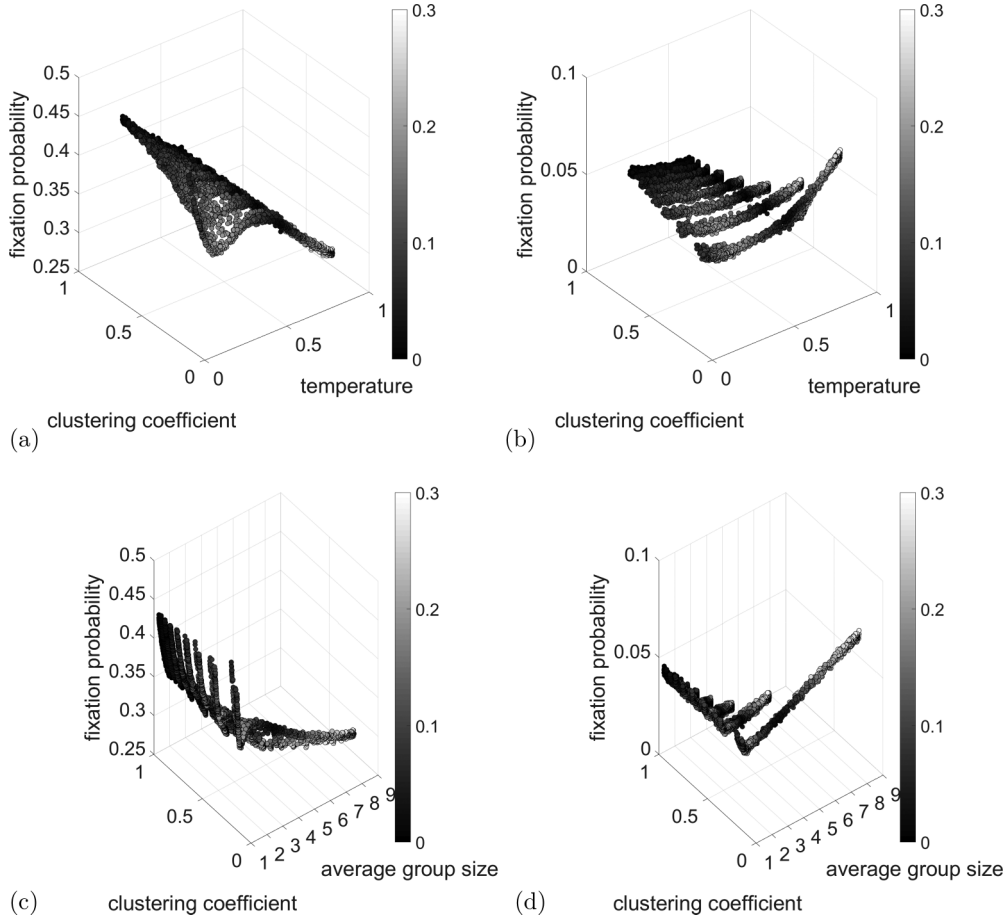
FIG. 12. Three-dimensional figure for the fixation probability as a function of clustering coefficient and temperature [(a) public goods game, (b) hawk-dove game] and average group size [(c) public goods game, (d) hawk-dove game] with a closer look at the standard deviation of node temperature (see the vertical bar accompanying each figure), with D invading C and D invading H.

a lower clustering coefficient again favors doves as we see in Fig. 10(a). However, for defectors, this effect is reversed with a higher clustering coefficient favoring defectors, since the smaller group size means there is a greater probability of being a lone individual.

In summary, the Barabási-Albert model is the only one to allow temperatures significantly higher than those found in well-mixed populations, considering the size of the network used in this paper. The preferential attachment rule of the model allows the network to have a small number of highly connected nodes, which return a higher average group size. The networks with few connections have low clustering coefficient and the widest temperature range. Small groups favor hawks invading doves and defectors invading cooperators (the small groups should be bigger than 1 to favor the hawks). Since the Barabási-Albert network allows large groups, it favors doves invading hawks and decreases the fixation probability for defectors invading cooperators.

V. DISCUSSION

In this paper, we have built on the existing framework of Broom and Rychtář [26], in particular investigating factors that determine the fixation probability of mutants using their territorial raider model for a large range of different popula-

tion structures. This model is built on an underlying network structure, and we used five types of complex networks: Erdös-Renyi (random), small-world, scale-free, Barábasi-Albert, and random regular networks. We also considered a number of population properties in conjunction with these networks; these were five topological parameters of the generated networks: average degree, clustering coefficient, shortest path, density, and diameter, together with the graphical temperature (using the replacement weight matrix), the mean group size, and the model's "home fidelity" parameter.

The main objective of the paper was to find population properties that could predict the fixation probability. The topological parameters were poor predictors, and out of the other factors, the graphical temperature was the best predictor, as also found in previous work on very small networks [36], and average group size was also a strong predictor. In addition, the clustering coefficient proved to be a useful secondary predictor, in conjunction with the others.

The predictions of our model are often in accord with those from classical evolutionary graph theory. Populations structured over star networks tend to favor doves invading hawks due to large groups [1], and we also have this effect for small networks [36]. In [29], the wealth distribution model using the public goods game found that stars increase the inequality in the population due to a better situation for defectors. In [11],

scale-free networks were the hottest network in the paper, and the hottest cases were where the doves performed better. We note that the linear relationship with mean temperature is new; typically evolutionary graph theory models exclude self-weights, and then the mean temperature is just 1 for all graphs (for some consequences of including self-weights in evolutionary graph theory, see [44]). A similar relationship with a differently defined temperature can be seen in [57] for a model of a finite well-mixed population.

This similarity of predictions is not surprising, as both models are built on sensible assumptions that are realistic for nonextreme situations (e.g., graphs that are close to being well mixed). There are some phenomena that we have observed in our model that have not been observed for evolutionary graph theory, however, in particular the results from Sec. IV B where we discuss unusual features of our plots, including the turning point in the graphs with high temperatures and the plots where for some temperatures there are multiple trend lines associated with different clustering coefficients. These features occur for graphs that are in some sense extreme, with the potential for very high temperatures and group sizes, and it is in such graphs that the assumptions of our model and those of classical evolutionary graph theory differ most. When large groups can form, the nonlinearity of our model and the payoffs of the constituent games are most in evidence.

In general, an important feature of our model is the existence of variable group sizes, which is a realistic feature absent from evolutionary graph theory models. The fact that evolutionary graph theory and our more involved framework often yield similar results can be argued as a case of the simpler model being sufficient to make good predictions in a range of circumstances, just as well-mixed populations from classical evolutionary game theory give results close to evolutionary graph theory in general, and only when the structural component is significant do the advantages of the evolutionary graph theory methodology become apparent. In the same way, it is when structure would yield significantly variable group sizes, and in particular large groups, that evolutionary graph theory models do not produce the predictions that our methodology does.

The variability of group sizes includes the possibility of being alone. Thus how we define the payoff for being alone can have a significant effect, especially when mean group sizes are small, as we have mentioned in Sec. II D 2. We note that it would be possible to consider lone individuals in evolutionary graph theory too by introducing self-loops within the graph, and the likelihood of individual interactions could be decided by choosing an appropriate weight to this link. The public goods game considered also has a maximum payoff of V, irrespective of how many cooperators there are. Alternative games could thus yield a stronger effect of group size overall. We note that there are many different multiplayer games that we could use, including different types of public goods games, and we consider these, and the effect of different mean group sizes, in the paper [58]. In fact the discussion about the effect of individuals being alone can in one sense be seen as a strength of our work. Lone individuals arise naturally as part of our framework, and we would argue that this important feature has often been lost due to the imposition of pairwise models for all interactions.

An interesting feature of our results is that for the public goods game, the fixation probability of defectors has a decreasing trend with the average group size. At first sight this contradicts earlier work where the defectors' fixation probability increased with the group size as in [37] or [33]. A key difference here is that in the above work the group sizes were fixed, or the variability of the group sizes was low (in the case of [37]). Here we have very variable group sizes, with a significant probability of lone individuals. This particularly affects the initial trend for small mean group sizes as defectors do well for lone individuals, and cooperators do especially well for actual (as opposed to mean) group size two (again see [37]). We can see from the Figs. 7(d) and 7(e) that the trend is initially steep but flattens down. In our version of the public goods game, lone cooperators still pay a cost. We have checked an alternative version of the game where they do not (figure not shown). In that version, the trend is reverted, and we observe a clear increase in the fixation probability with the mean group size, for all group sizes.

The existence of lone individuals is not completely the answer, as the trend does keep decreasing even for quite large group sizes. The variability of the group sizes itself is an important factor here. A common (but definitely not universal) feature of variable group sizes (see [58], which considered a range of multiplayer games) is that the more variable the group size, the better the cooperators perform relative to the defectors (in particular the larger the incentive function, the larger the payoff to a cooperator minus that to a defector). As group sizes go up for our model both mean and variance increase, so that these effects pull in opposite directions. In general specific choice of game, underlying graph, dynamics, and variability of group size will all have an effect on this issue.

Although the temperature (and to a lesser extent group size) is a good predictor of the fixation probability, an interesting result is the nonmonotonic trend found on scale-free and Barábasi-Albert networks for the hawk-dove game. Moreover, the temperature has values higher than for the completely mixed case only for these networks, and the turning point in the trend happened at around the completely mixed temperature of 0.632. For these cases, consideration of the clustering coefficient helped us to understand that the concentration of connections to a small number of nodes enables "hotter" networks that suppresses selection. In particular, when the clustering coefficient is low, there could be a marked deviated from the trend as observed in the figures.

Moreover, the proposed numerical methodology is an alternative to deal efficiently with large networks. The system of linear equations grows exponentially with the number of nodes [36,59], and considering the large number of different networks treated here, an analytical resolution would be arduous. The methodology used here can be applied to consider models from the framework of [26] even for much larger populations. Therefore, this framework can be computationally optimized to deal with even larger populations.

There are a number of promising directions for future work. In previous work, especially [36], we have only considered this model for relatively small networks, and while our results are consistent with the earlier ones, consideration of many larger networks has enabled a clearer pattern, and also unusual features, to emerge. In future work we will explore

these various patterns in more detail, and also consider the effect of different dynamics on the fixation probability. We can apply the methodology for larger networks as described above. Although the simulations for 20 nodes took about 1100 hours to complete on a PC with 4.4 GHz and 16 GB RAM, increasing the size of the network would result in a wider range of parameters, and it would be interesting to see whether the trend change found for scale-free networks would be similar to the Barábasi-Albert case. We use an infrastructure for parallel computation, which reduced the simulation time by approximately 70%.

Can we combine the existing predictors, temperature, mean group size, and clustering coefficient to provide a more effective single predictor? Can we find other additional secondary predictors, that in combination with the existing predictors, especially the temperature, provide even more effective predictors?

There are a number of different evolutionary dynamics that can be applied, as detailed in [37], and it is important to see what predictive factors are needed for these alternative dynamics; for example, will a different type of temperature be needed in some cases? It is known that different dynamics can have a big effect in evolutionary graph theory, and that is also true in this framework, as seen in [37].

Predicting network properties is a relevant problem in different areas. In evolutionary graph theory, the graph structures that promote the evolution of cooperation have been extensively analyzed, for instance, using direct reciprocity on graphs [60] and directed networks [61]. Recently, [62] considered linking together structures that are unpromising for cooperation to produce an overall structure that favors it; this is a similar effect to that from our more extreme Barabási-Albert networks that generate a small number of separate clusters. Related problems consider the evolution of social behavior [34] and spatial evolutionary games [14,15,17,63–65].

[1] E. Lieberman, C. Hauert, and M. Nowak, Nature (London) **433**, 312 (2005).

[2] T. Antal and I. Scheuring, Bull. Math. Biol. **68**, 1923 (2006).

[3] M. Nowak, *Evolutionary Dynamics: Exploring the Equations of Life* (Harvard University Press, Cambridge, MA, 2006).

[4] M. Broom and J. Rychtář, Proc. R. Soc. London A **464**, 2609 (2008).

[5] B. Voorhees and A. Murray, Proc. R. Soc. London A **469**, 20120676 (2013).

[6] W. Maciejewski, F. Fu, and C. Hauert, PLoS Comput. Biol. **10**, e1003567 (2014).

[7] L. M. Ying, J. Zhou, M. Tang, S. G. Guan, and Y. Zou, Front. Phys. **13**, 130201 (2018).

[8] J. Maynard Smith, *Evolution and the Theory of Games* (Cambridge University Press, Cambridge, UK, 1982).

[9] J. Hofbauer and K. Sigmund, *Evolutionary Games and Population Dynamics* (Cambridge University Press, Cambridge, UK, 1998).

[10] M. Broom and J. Rychtář, *Game-Theoretical Models in Biology* (CRC Press, Boca Raton, FL, 2013).

[11] H. Ohtsuki, C. Hauert, E. Lieberman, and M. A. Nowak, Nature (London) **441**, 502 (2006).

[12] F. Santos and J. Pacheco, J. Evol. Biol. **19**, 726 (2006).

[13] C. Hadjichrysanthou, M. Broom, and J. Rychtář, Dynamic Games and Applications **1**, 386 (2011).

[14] M. Nowak and R. May, Nature (London) **359**, 826 (1992).

[15] M. Nowak and R. May, Int. J. Bifurcation Chaos **3**, 35 (1993).

[16] M. Schaffer, J. Theor. Biol. **132**, 469 (1988).

[17] T. Killingback and M. Doebeli, Proc. R. Soc. London B **263**, 1135 (1996).

[18] A. Li, B. Wu, and L. Wang, Sci. Rep. **4**, 5536 (2014).

[19] J. Ginsberg and D. Macdonald, *Foxes, Wolves, Jackals, and Dogs: An Action Plan for the Conservation of Canids* (IUNC, Gland, Switzerland, 1990).

[20] S. Kelley, D. Ransom Jr., J. Butcher, G. Schulz, B. Surber, W. Pinchak, C. Santamaria, and L. Hurtado, Journal of Field Ornithology **82**, 165 (2011).

[21] G. Palm, J. Math. Biol. **19**, 329 (1984).

[22] M. Broom, C. Cannings, and G. Vickers, Bull. Math. Biol. **59**, 931 (1997).

[23] M. Bukowski and J. Miekisz, Int. J. Game Theory **33**, 41 (2004).

[24] C. Gokhale and A. Traulsen, Proc. Natl. Acad. Sci. USA **107**, 5500 (2010).

[25] C. Gokhale and A. Traulsen, Dynamic Games and Applications **4**, 468 (2014).

[26] M. Broom and J. Rychtář, J. Theor. Biol. **302**, 70 (2012).

[27] C. Hauert, S. De Monte, J. Hofbauer, and K. Sigmund, Science **296**, 1129 (2002).

[28] M. Milinski, D. Semmann, H. Krambeck, and J. Marotzke, Proc. Natl. Acad. Sci. USA **103**, 3994 (2006).

[29] F. C. Santos, M. D. Santos, and J. M. Pacheco, Nature (London) **454**, 213 (2008).

[30] S. Kurokawa and Y. Ihara, Proc. R. Soc. London, Ser. B **276**, 1379 (2009).

[31] M. Souza, J. Pacheco, and F. Santos, J. Theor. Biol. **260**, 581 (2009).

[32] F. Santos and J. Pacheco, Proc. Natl. Acad. Sci. USA **108**, 10421 (2011).

[33] M. van Veelen and M. Nowak, J. Theor. Biol. **292**, 116 (2012).

[34] S. Kurokawa and Y. Ihara, Theoretical Population Biology **84**, 1 (2013).

[35] M. Bruni, M. Broom, and J. Rychtář, Involve, J. Math. **7**, 129 (2014).

[36] M. Broom, C. Lafaye, K. Pattni, and J. Rychtář, J. Math. Biol. **71**, 1551 (2015).

[37] K. Pattni, M. Broom, and J. Rychtář, J. Theor. Biol. **425**, 105 (2017).

[38] K. Pattni, M. Broom, and J. Rychtář, Discrete and Continuous Dynamical Systems, B **23**, 1975 (2018).

[39] N. Galanter, D. Silva, J. T. Rowell, and J. Rychtář, J. Theor. Biol. **412**, 100 (2017).

[40] F. Débarre, C. Hauert, and M. Doebeli, Nat. Commun. **5**, 3409 (2014).

[41] A. McAvoy and C. Hauert, J. R. Soc., Interface **12**, 20150420 (2015).

[42] S. Boccaletti, V. Latora, Y. Moreno, M. Chavez, and D. U. Hwang, Phys. Rep. **424**, 175 (2006).

[43] L. Hindersin, M. Möller, A. Traulsen, and B. Bauer, BioSystems **150**, 87 (2016).

[44] K. Pattni, M. Broom, J. Rychtář, and L. J. Silvers, Proc. R. Soc. London A **471**, 20150334 (2015).

[45] C. Hauert and G. Szabó, Complexity **8**, 31 (2003).

[46] P. Erdos and A. Rényi, Publicationes Mathematicae **6**, 290 (1959).

[47] D. Watts and S. Strogatz, Nature (London) **393**, 440 (1998).

[48] R. Albert and A. L. Barabasi, Rev. Mod. Phys. **74**, 47 (2002).

[49] M. Newman, *Networks: An Introduction* (Oxford University Press, New York, NY, 2010).

[50] B. Bollobás, O. Riordan, J. Spencer, and G. Tusnády, Random Struct. Alg. **18**, 279 (2001).

[51] A.-L. Barabási and R. Albert, Science **286**, 509 (1999).

[52] G. Csardi and T. Nepusz, InterJournal, Complex Syst. **2006**, 1695 (2006).

[53] K.-I. Goh, B. Kahng, and D. Kim, Phys. Rev. Lett. **87**, 278701 (2001).

[54] B. Adlam, K. Chatterjee, and M. A. Nowak, Proc. R. Soc. London A **471**, 20150114 (2015).

[55] B. Allen, A. Traulsen, C. Tarnita, and M. Nowak, J. Theor. Biol. **299**, 97 (2012).

[56] J. Peña and G. Nöldeke, J. Theor. Biol. **389**, 72 (2016).

[57] A. Traulsen, M. A. Nowak, and J. M. Pacheco, J. Theor. Biol. **244**, 349 (2007).

[58] M. Broom, K. Pattni, and J. Rychtář, Bull. Math. Biol., doi:10.1007/s11538-018-00545-1 (2018).

[59] M. Broom, C. Hadjichrysanthou, and J. Rychtář, Proc. R. Soc. London A **466**, 20090487 (2009).

[60] H. Ohtsuki and M. A. Nowak, J. Theor. Biol. **247**, 462 (2007).

[61] N. Masuda and H. Ohtsuki, New J. Phys. **11**, 033012 (2009).

[62] B. Fotouhi, N. Momeni, B. Allen, and M. A. Nowak, Nature Human Behaviour **2**, 492 (2018).

[63] B. Allen, J. Gore, and M. A. Nowak, eLife **2**, e01169 (2013).

[64] J. Peña, G. Nöldeke, and L. Lehmann, J. Theor. Biol. **382**, 122 (2015).

[65] A. Szolnoki and M. Perc, Phys. Rev. E **81**, 057101 (2010).